Chapter 1

Introduction: Concepts of Extragalactic Astrophysics

1.1 The Scale of the Universe

Ever since the cosmos have been observed by humanity, new insights in the nature of the universe have been forming the human view of the world. The human mind and

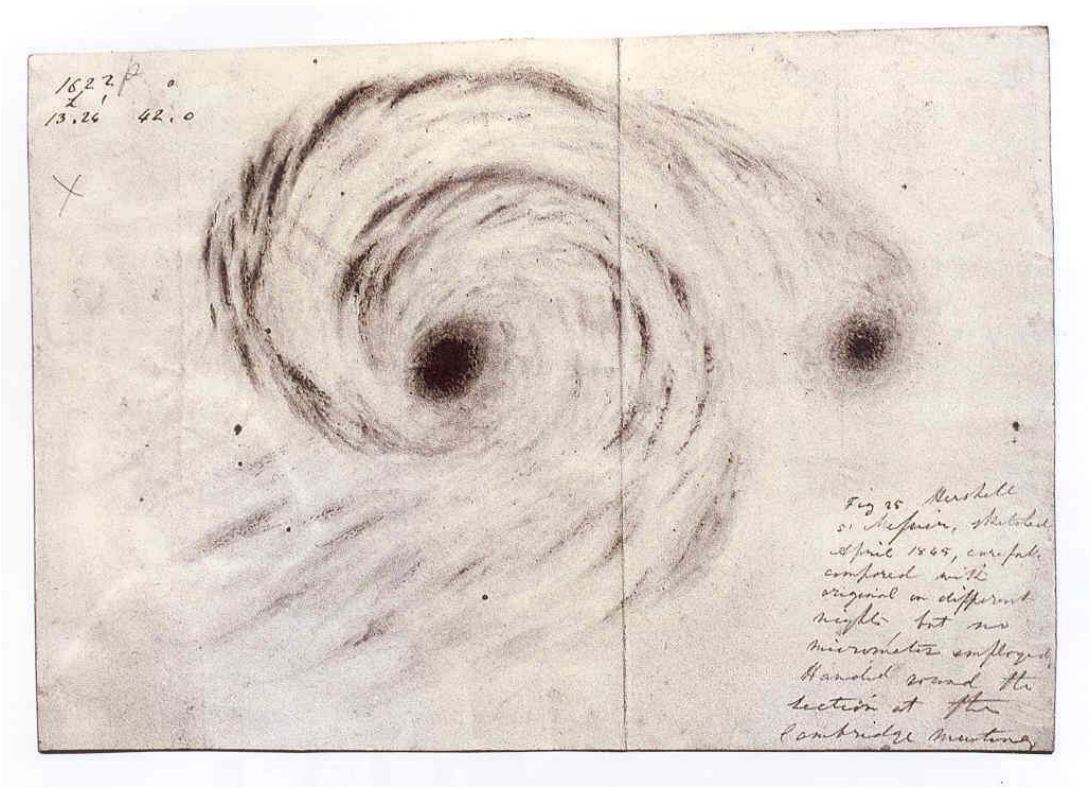

FIGURE 1.1: One of the first drawings of a spiral nebula by Lord William Henry Parsons as seen through the 'Leviathan of Parsonstown' telescope in 1845.

its capability to understand and interpret cosmic facts and processes have always been limited by the resolution of technical resources. Until the modern age, these resources have been restricted to the human eye and our location has been believed to be a privileged, central position in this human view of the world. However, even in ancient Greece, the philosopher Democritus ($450 - 370\,BC$) proposed that the visible part of our local host galaxy, the Milky Way, is a large accumulation of stars like the sun.

The first use of optical instruments heralded the Copernican Turn. In the early 17^{th} century, one of the first telescopes was used by Galileo Galilei (1564–1642) in order to resolve fainter, stellar sources in the Milky Way beyond the possibilities of the human eye. The result confirmed the suggestion of Democritus, that our host star, the Sun, is a small part of a huge stellar network. In addition to this observation, the Copernican Turn proved that our location in the universe is neither central, nor extraordinary in any geometrical sense.

Further details on the nature of galaxies and the location of the Earth in the universe have been postulated by Giordano Brunoin (1548–1600) in the 16^{th} century and by Thomas Wright (1711–1786). In 1750, Wright postulated in his eminent seminal study "`An original theory or new hypothesis of the universe`" one of the first predictions on the true nature of galaxies and identified the observed mysterious nebulae as incredibly distant galaxies. In addition, Wright identified the disk of the Milky Way as an accumulation of "stars in a flat layer" with the sun inside its plane. Interceder of Wright's ideas, the philosopher Immanuel Kant (1724–1804) and others, first identified the observed, unclear nebulae as systems of stars and called them 'Island Universes'. The first maps and catalogues of extragalactic nebulae have been provided by Charles Messier (1730–1817) and by William Herschel (1738–1822) in the 2^{nd} half of the 18^{th} century. Expanding on Messier's catalogue, Herschel provided the first known atlas of extragalactic sources with more than 5000 galactic nebulas in 1785.

Remarkable improvements in the optical instrumentation were reached in the mid 19^{th} century with the construction of the telescope 'Leviathan of Parsonstown' by Lord William Henry Parsons in Ireland [South, 1845]. Equipped with a large mirror (1.8 m), it was first possible to resolve the spiral structure (Parsons, 1845) of the neighbouring galaxy Messier 51 (M51) and the first galaxy merger was observed, although it was not identified as such. Fig. 1.1 shows one of the first drawings of M51, the first observation of a spiral nebula, as presented at the meeting of the British Association for the Advancement of Science in 1845. With this new, unforeseen telescope resolution it was possible to divide galaxies into elliptical and spiral nebula; the early era of galaxy morphologies had begun. Although the telescope was able to resolve single stars [Parsons, 1850], the true nature of the observed stellar nebula still remained unclear.

In the following decades, spectroscopic analysis provided velocity measurements of neighbouring spiral nebula [Slipher, 1915]. The first analysis of the radial Doppler shift velocity for the nearby Andromeda galaxy [Slipher, 1913] and an additional sample of 15 spiral galaxies gave another hint on the extragalactic nature of the observed nebula. From this analysis, it was concluded that the observed nebulas were estimated to be on average 25 times faster as the average stellar velocity of usual stars in the Milky Way.

Nearly two centuries after the theories of Thomas Wright and Immanuel Kant, these remarkable results re–inspired their postulations and initiated one the most important milestones in astronomy and the human view of the world: The Great Debate. In 1920, the astronomers Harlow Shapley (1885–1972) and Heber Doust Curtis (1872–1942) suggested two scenarios in order explain the true nature of the observed stellar nebulas. These ideas were presented in their common paper "The Scale of the Universe". Shapley suggested that the Milky Way was indeed bigger than previously assumed and that it contained the spiral nebula. Curtis advocated the postulations of Wright and Kant, that Andromeda, M51 and other observed spiral nebulas are indeed "World Islands" and extra–galactic sources. He argued that the observed rate of supernovae in the nebular systems is abnormally high in comparison with any other known objects in the Milky Way.

However, the Great Debate still separated the positions of astronomers for several years, but it pointed to ask the right questions. A first, appropriate estimation for distance to the neighbouring galaxies Andromeda (M31), the Barnard's Galaxy (NGC 6822), and Triangulum (M33) was provided by Edwin Hubble. Observations of periodic changes in the luminosity of bright, extra–galactic Cepheid stars were used in order to estimate the absolute magnitudes of the stellar sources with the period–luminosity relation for Cepheid stars [Shapley, 1922, see also Eq. 1.1].

$$M = -2.81 \cdot \log \frac{\mathrm{P}}{\mathrm{days}} - 1.43 \tag{1.1}$$

This empirical approximation describes a relation between the absolute magnitude M and the periodic change P in days of the luminosity of Cepheid stars. As a consequence, it became possible to estimate the distances to the observed light sources based on well–known magnitude–distance relations. Finally, the questions of the Great Debate were undoubtedly answered by the cosmic distance relations of the observed sources by Edwin Hubble. It turned out that galaxies are indeed gravitationally bound structures of stars, dust, gas, planetary systems and other stellar objects at incredibly large distances from the Earth. The observed, extragalactic nebular structures have from now on been

divided into elliptical and spiral galaxies. In addition, galaxies have been arranged into several morphological types (see Sect. 1.2, The Hubble Tuning Fork).

The first evidence for the existence and the true nature of galaxies led to a new era in extragalactic astronomy and cosmology. Hubble's spectroscopic measurements provided additional information in order to point to new questions in cosmology about the formation and the evolution of the universe. Solar–corrected, radial velocities have been measured for a sample of 22 nearby galaxies [Hubble, 1929] and gave a first hint on the modern conception of the expanding universe. The result of Hubble's measurement of the distance and radial velocity was Hubble's Law (Eq. 1.2), which is fundamental in our understanding of the expanding universe.

$$v = H_0 \cdot d \tag{1.2}$$

$$H_0 = (74.3 \ \pm 2.1)\,\mathrm{kms}^{-1}\mathrm{Mpc}^{-1} \tag{1.3}$$

Here, the Hubble parameter H_0 is describing the present expansion rate of the universe (see Eq. 1.3). It relates the recessional velocity v with the proper distance d of a galaxy to the observer. As a direct consequence, the first description of a time–dependent evolution of the expanding universe as previously predicted by Lemaitre [1931] have now been further supported and the Big Bang Theory was born.

In order to explain a number of subsequent observations, however, additional physical concepts were required. The gravitational forces which are caused only by the visible and detectable mass have not been sufficient in order to explain the observed object trajectories and galaxy structures. Hence, the current physical standard model of cosmology includes the additional concept of *dark matter*. Gravitational effects, the cosmic microwave background (for an illustration see Fig. 1.8) and additional evidence from the Big Bang nucleosynthesis suggest that only $\sim 4\%$ of the matter in the universe consist of baryonic matter. The particle physical nature of dark matter remains unknown and dark matter has never been measured directly. As the distribution of dark matter in the universe is correlated with presence of galaxies, galaxies provide an important tracer for the study of dark matter and its role in the formation and evolution of the universe.

In the course of the present scientific results of extra–galactic astronomy, many questions still remain debated and a complete, unified model which explains the morphological structure of galaxies still does not exist. Physical processes and drivers of galaxy

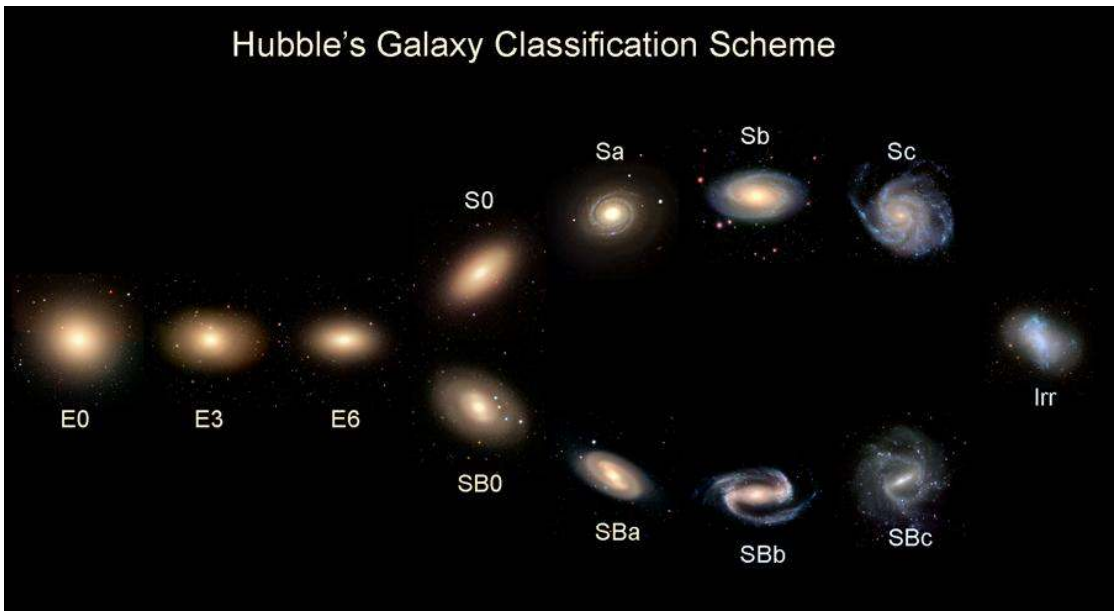

FIGURE 1.2: The Hubble Tuning Fork, a classification scheme for galaxies according to their morphologies. Elliptical galaxies (E) with different ellipticities are shown on the left and spiral galaxies (S) with bulges and disks are arranged in the right branches. Lenticular galaxies (S0) with a featureless disk are in the middle. The branches distinguish between barred (B) and non–barred systems. Irregular galaxies (Irr) are not included. The stellar populations are reflected in the colors of the galaxies: Red galaxies and galaxy components mainly consist of red and old stellar populations, whereas the light in the blue disks is dominated by younger stellar populations in actively star forming regions.

evolution still remain only tentatively answered or are even contradictory. A contemporary and increasingly popular means by which to tackle this subject is via the analysis of large, automatically produced datasets containing robust morphological parameters. One such implementation is GALAPAGOS-C.

1.2 Galaxy Morphologies

Morphology is a general term for the shape and the distribution of light sources and light intensity within an astronomical source. Most of the classification schemes divide galaxies into elliptical, spiral and irregular types. The most prominent classification scheme is the Hubble Tuning Fork, which was first presented by Hubble [1927]. More recent approaches for the classification of galaxies include additional information on the galaxy components, peculiarities or asymmetrical features.

1.2.1 The Hubble Tuning Fork

In the 1920s, further improvements in the resolution of optical devices permitted deeper insights into the morphologies of galaxies and their sub–structures. Galactic bulges, spiral arms and bars have been resolved and the previously existing, detailed galaxy catalogues [Dreyer, 1888, Herschel, 1864] have been expanding accordingly.

The Hubble Tuning Fork (also Hubble Sequence) is a classification scheme for galaxies and remains one of the most successful approaches until today (see Fig. 1.2). On the left side, smooth, elliptical galaxies which mostly consist of a single, reddish component are arranged. As we move to the right, the elliptical galaxies become more elongated. The galaxies on the right consist of several components: A red and roundish bulge component is found in the centre for most of the galaxies. In addition, the galaxies on the right hand side contain disks with different relative sizes in comparison to the bulge. In spiral galaxies, the disk contains distinct spiral arms, whereas lenticular (also S0) galaxies contain a featureless disk. Disk galaxies sometimes contain an elongated, roundish bar component in the centre (lower branch). Lenticular galaxies can exist both with and without a bar. At the same time, however, a significant fraction of galaxy types with additional features and irregularities (e.g. galaxies with ring structures) cannot be included in this diagram. The relative size of the bulges decrease from left to right and the spiral arms become more distinct open wound. In practice, the described galaxies can also occur as a mixture of two or more neighbouring galaxy types and, in addition, often show peculiar features.

In general linguistic usage, the misleading notation “early–type galaxies” is used for ellipticals and “late–type galaxies” is used for objects with a prominent disk. In fact, the Hubble Sequence does not intend any temporal evolution scenario for galaxies and their morphologies.

1.2.2 Adaptations of the Hubble Tuning Fork

The Hubble Tuning Fork is a first approach in order to classify the various types of galaxies. The full range of galaxy morphologies, galaxy types and additional structural components, e.g. rings or lenses, is not described or included adequately. A widely–used extension to the Hubble Tuning Fork is the system by de Vaucouleurs [1963]. In addition to Hubble’s basic division into elliptical, lenticular, spiral and barred spiral galaxies, the de Vaucouleurs system introduces a more elaborate classification system by adding three additional morphological components: First the morphology of **bars** is more emphasized in the de Vaucouleurs system. It still divides between barred (B) and

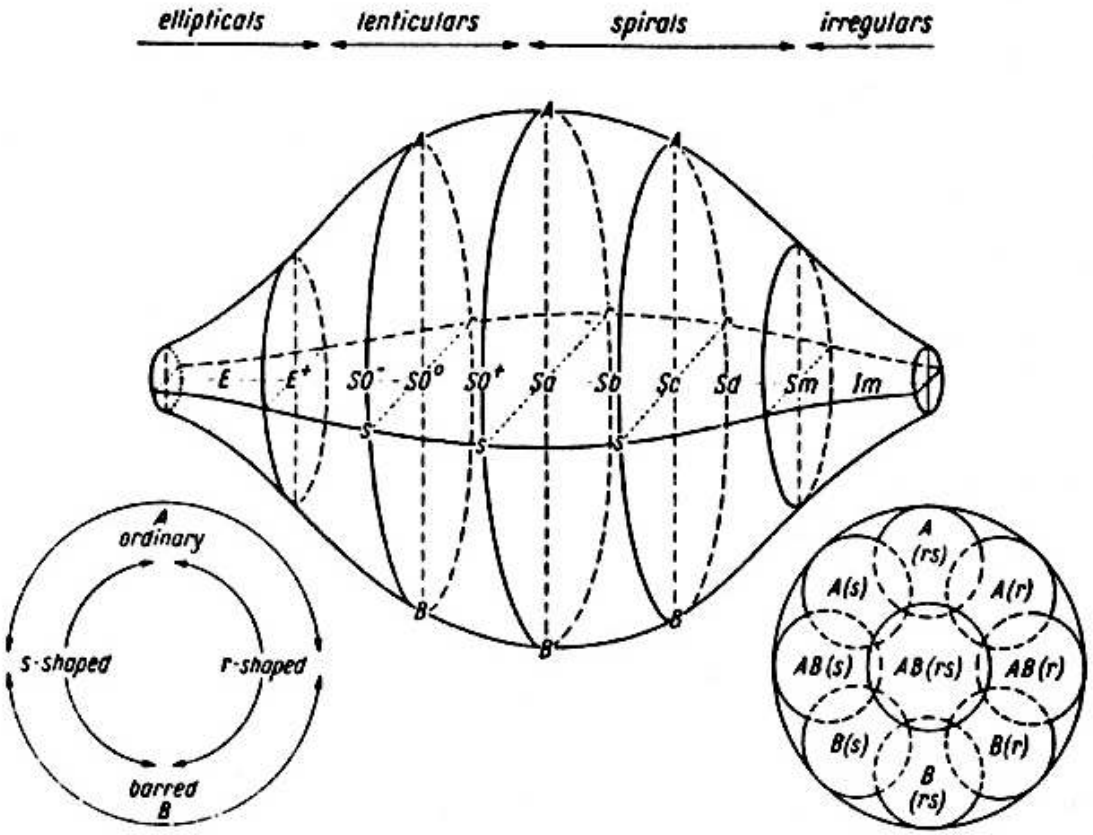

FIGURE 1.3: A three–dimensional extension of the Hubble Tuning Fork by de Vaucouleurs [1963]. The x–axis indicates the basic morphological type of a galaxy. The y–axis provides information on the presence or absence of a bar and the z–axis indicates the presence or absence of a ring. Additional emphasis is put on the relative bulge–to–disk ratios of lenticular galaxies and intermediate types. The lower figures provide denotation keys for barred (B) and non–barred (A) galaxies and for ring galaxies (r) and galaxies without a ring (s). In addition, it allows for less prominent or transition states for bars (AB) and for rings (rs).

non–barred (A) galaxies, but allows for an intermediate type (AB) for galaxies with a weak bar or a transition state. Second, it provides information about galaxies with a **ring** (r) and without rings (s) and an intermediate or transition state (rs) can be co–added. Third, several **additional spiral classes** are added to the Hubble Tuning Fork in order to classify irregulars or galaxies with a distorted morphology more accurately. The Sd (SBd) class refers to galaxies with diffuse arms, nebular structures and a very faint or no bulge. The Sm (SBm) refers to irregular galaxies with a spiral feature and the Im class represents completely irregular galaxies. Additionally, the relative development of the disk component for lenticular galaxies is described more in detail as suggested by Holmberg [1958]. The notation E^+, $S0^-$, $S0^0$, $S0^+$ provides information about the relative importance of the disk from high to low bulge–to–disk ratios. The de Vaucouleurs system combines the above mentioned notations. As indicated in Fig. 1.3, it describes the Hubble Tuning Fork in a three–dimensional way. Similar to the Hubble

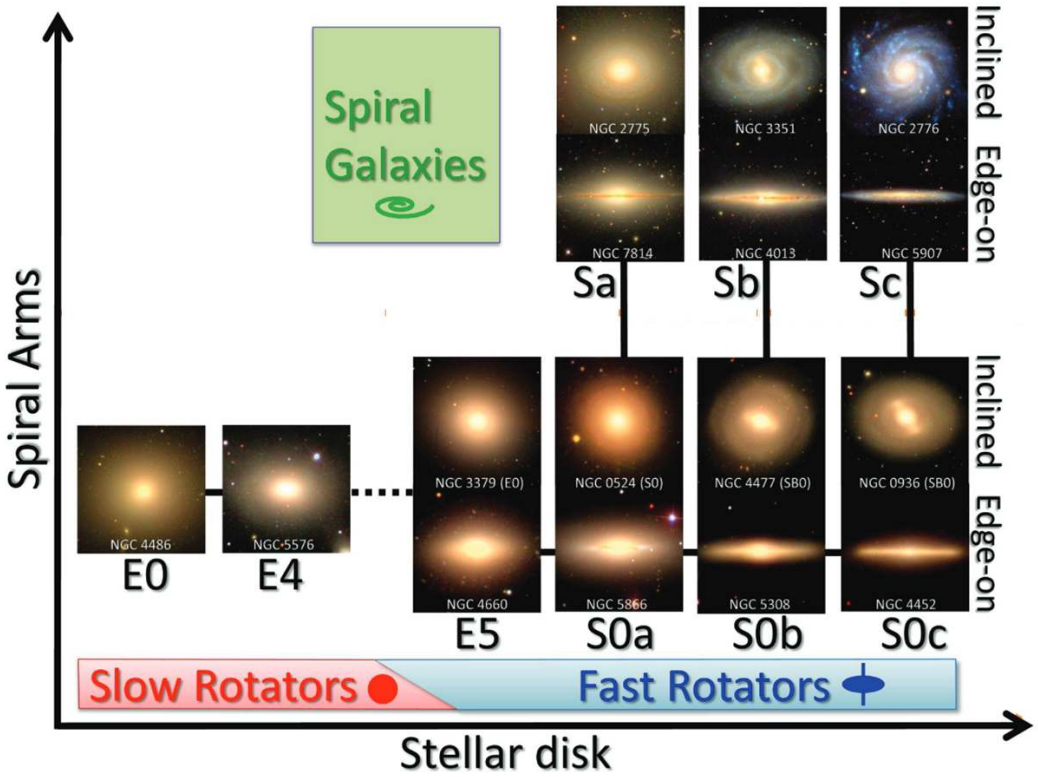

FIGURE 1.4: A revision of the Hubble Tuning Fork from Cappellari et al. [2011]. As in the Hubble Tuning Fork, the relative size of the stellar disk is indicated by the x–axis. Additional emphasis is put on the shape of the spiral arms with more distinct arms on the upper y–axis. Furthermore, it provides information about average properties of galaxies which are statistically correlated with the morphology, e.g. slow rotating galaxies on the left and fast rotators on the right, galaxies with high mass–to–light ratio at the bottom and large galaxies with a high amount of gas and active star formation at the top.

Tuning Fork, the x–axis refers to the stage (spiralness) of the galaxy and the family (barredness) is indicated on the y–axis. In addition, it refers to the variety (ringness) on the z–axis [de Vaucouleurs, 1963].

Further adaptations and revisions of the Hubble Tuning Fork have been presented e.g. by Cappellari et al. [2011] in 2011 or by Kormendy and Bender [2012] in 2012. An additional morphological property of elliptical galaxies is the structure of the isophotes with disky and boxy shapes. In contrast to the true ellipticity of an elliptical galaxy, the structure of the isophotes is more independent from the relative inclination angle towards the observer. To this end, the latest revisions of the Hubble Tuning Fork order the early–type arm according to the isophotal shape of the elliptical galaxies. Each elliptical galaxy is characterized by an addition of (b) for boxy ellipticals or (d) for disky shapes. According to van den Bergh [1976], the relative bulge–to–disk sizes for lenticular galaxies are even more emphasized in the latest classification systems in comparison to

the de Vaucouleurs revision of the Hubble Tuning Fork with decreasing bulge–to–disk ratios from left to right.

In Fig. 1.4, Cappellari et al. [2011] provide an additional revision of the Hubble Tuning Fork. The x–axis describes how distinct the stellar disk is, with bulge–dominated galaxies on the left and disk–dominated systems on the right. The y–axis provides information about the presence or absence of spiral arms or a dust lane. Galaxies with a dust lane and distinct spiral arms are on top, elliptical and lenticular types with no prominent spiral arms are on the bottom. Additionally, this classification scheme emphasizes the correlation of kinematic features with morphological structures for slow and fast rotating galaxies. On average, the rotation velocity increases towards later, disk–dominated galaxy types. While the galaxy size and gas content increase as one goes to galaxies with prominent spiral arms, the mass–to–light ratio will decrease.

The described galaxy classification schemes mostly refer to giant galaxy types. More detailed observation and high resolution surveys provide additional information on smaller and fainter types. One of the first extensions to the discussed classification schemes including dwarf galaxies was presented by Sandage and Binggeli [1984]. Dwarf elliptical galaxies (dE) and dwarf lenticulars (dS0) are included into the classification schemes as a subsequent extension to their giant counterparts. In addition, disturbed elliptical galaxies (dEpec) are included. Apart from single observations, the wide existence of dwarf spiral galaxies is still in debate [e.g. Jerjen et al., 2000]. Several sub–classes of small and faint galaxy types (e.g. Green Pea galaxies [Amorin et al., 2012], Blue Compact Dwarfs) are not yet discretely mentioned in any of these classification schemes. Peculiar galaxies and transition states like unusual dusty red spirals [e.g. Boesch et al., 2013, Wolf et al., 2003], dusty ellipticals [e.g. Rowlands et al., 2012] or blue ellipticals [e.g. Schawinski et al., 2009] still do not find their separate position in any classification scheme.

1.2.3 Galaxy Profiles

Since the era of the first photographic plates, the radial light profiles of galaxies have been approximated with analytical functions. The technique of parametric fitting was first applied by de Vaucouleurs [1948]. The first result has been that the light profiles of elliptical galaxies tend to be approximated with a exponential power–law according to $exp(r^{-1/4})$.

This detailed quantification of surface brightness profiles in a reproducible, mathematical way is an additional tool in order to provide additional insights into the intrinsic properties of galaxies as they are often correlated with the morphological type [e.g.

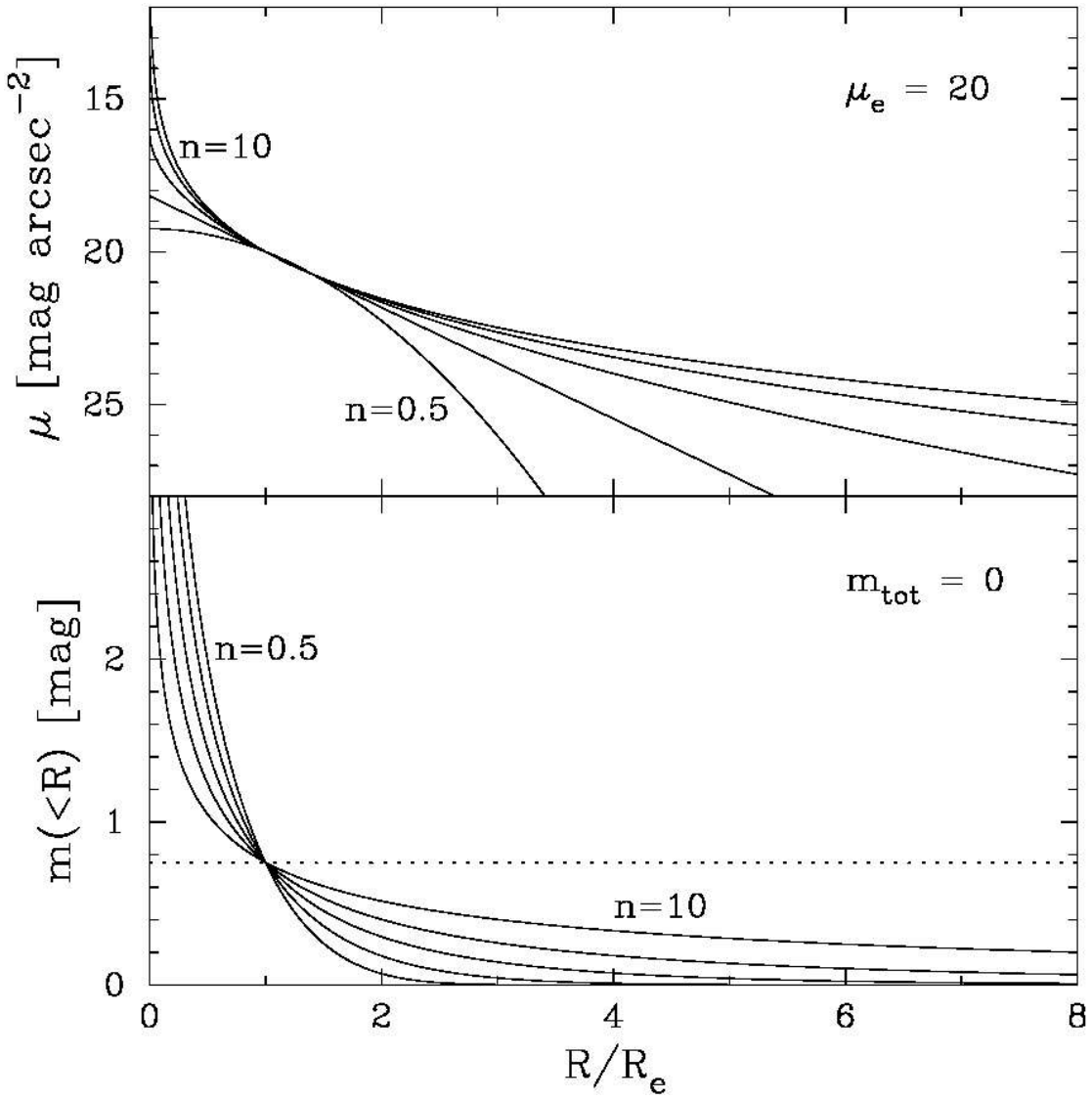

FIGURE 1.5: Single Sérsic surface brightness profiles (Equation 1.4) are shown in the top panel for the Sérsic indices n = 0.5, 1, 2, 4, and 10. The profiles are normalised at a surface brightness of $\mu = 20\,mag\,arcsec^{-2}$. In the lower panel, Sérsic aperture magnitude profiles are shown for the according profiles. The profiles are normalised so that the total magnitude is equal zero. The figure is adopted from Graham et al. [2005] and Kelvin et al. [2012].

Kartaltepe et al., 2014]. The classification according to the previously mentioned classification schemes is subjective and sometimes unclear even amongst experts. Hence, a significant fraction of the observed galaxies cannot be classified in an indisputable fashion. E.g. Naim et al. [1995] and Kelvin et al. [2012] describe that the uncertainties and the intrinsic scatter for the morphological galaxy classification according to Hubble types are non–negligible.

With improving data quality due to the use of charged coupled devices (CCDs), the fitting technique has been improved and the de Vaucouleurs profile has been replaced by a generalized $\exp(r^{-1/n})$ profile as first described by Sérsic [1968].

$$\Sigma(r) = \Sigma_e \exp\{-\kappa(n)[(r/r_e)^{(1/n)} - 1]\} \tag{1.4}$$

The Sérsic function describes galaxy profiles with a generalized approach. The surface brightness $\Sigma(r)$ is described as a function of radius r. Here, Σ_e is the effective surface brightness and r_e is the effective (or half–light) radius. However, the Sérsic index n is the most important parameter with $\kappa(n)$ as a normalization constant. According to the Sérsic index, the Sérsic profile is a generalized/transitional profile that is able to describe a de Vaucouleurs profile (with $n = 4$) or an exponential profile (with $n = 1$) for different types of galaxies as well as the galaxy components. Hence, the Sérsic index reflects the light concentration of a galaxy profile. A high Sérsicindex describes galaxies with a steep inner light profile and a pronounced light concentration in the central regions of the profile. Conversely, shallow profiles in the inner regions with a steep truncations at the boundaries are indicated by a low Sérsic index. The luminosity L which is encircled within a certain radius R can be calculated via integration:

$$L(< R) = \int_0^R \Sigma(R') 2\pi \, \mathrm{d}R' \tag{1.5}$$

In order to solve the integral, it is necessary to introduce the substitution $x = \kappa(n)(R/R_e)^{1/n}$.

Hence, the integrated luminosity is given by:

$$L(< R) = I_e R_e^2 2\pi n \frac{e^{\kappa(n)}}{(\kappa(n))^{2n}} \gamma(2n, x) \tag{1.6}$$

Here, $\gamma(2n, x)$ is the incomplete gamma function.

$$\gamma(2n, x) = \int_0^x e^{-t} t^{2n-1} \mathrm{d}t \tag{1.7}$$

The total luminosity in Eq. 1.6 is calculated by replacing the incomplete gamma function $\gamma(2n, x)$ with the complete gamma function $\Gamma(2n)$ [Ciotti, 1991]. Subsequently, the normalisation constant $\kappa(n)$ can be calculated according to:

$$\Gamma(2n) = 2\gamma(2n, x) \tag{1.8}$$

As a result, a common approximation of $\kappa(n)$ for $0.5 < \mathrm{n} < 10$ has been given by Prugniel and Simien [1997]:

$$\kappa(n) = 1.9992n - 0.3271 \tag{1.9}$$

Hence, established values for $\kappa(n)$ are $\kappa(1) = 1.678$ and $\kappa(4) = 7.669$. However, if n tends towards infinity, Ciotti and Bertin [1999] have shown that $\kappa(n) \mapsto 2n - 1/3$.

Fig. 1.5 shows an example for a Sérsic profile of a typical HST galaxy with different Sérsic indices in the upper panel. The higher the Sérsic index is, the more flux is concentrated in the central regions of the profile. At the same time, profiles with a high Sérsic index are more extended and cover a wide area of relatively low surface brightness at the outer regions. In the lower panel, Sérsic aperture magnitude profiles are shown for the associated profiles.

The Sérsic profile can be applied in order to describe entire galaxy profiles as well as several galaxy components. In 1970, one of the most important results in our understanding of galaxy structure was presented by Freeman [1970]. It was shown that the disk component can be remarkably well approximated with a pure exponential profile with a Sérsic index of $n = 1$, whereas the de Vaucouleurs profile provides a good approximation for the bulge component. In addition, e.g. Trujillo et al. [2001] provide information on the real truncations of the mathematically infinite profiles.

However, the Sérsic profile must be understood as a first–order approach, mainly because the central light concentrations in elliptical galaxies often undergo variations and must be described by a wider range of analytical profiles. In addition, for example Maltby et al. [2012] show that $\sim$50% of the observed disk galaxies in nearby galaxy clusters show profile truncations or anti–truncations in the outer disk regions.

1.2.4 Modern Galaxy Profile Quantification

In the last two decades, a set of automated tools and algorithms have been introduced in order to quantify galaxy morphologies with analytical profiles automatically. One of the first, widely–used algorithms is GIM2D [Simard, 1998]. GIM2D is applied to fit

two–dimensional light profiles to galaxies on an input image. In order to decompose galaxy profiles into a bulge and a disk component, it fits a sum of a Sérsic profile and a pure exponential profile (n = 1) to the input data. The structural parameters of each galaxy profile are stored in a catalogue.

In 2002, GALFIT [Peng et al., 2002] heralded the next generation galaxy fitting pipelines. In a similar way as GIM2D, minimization algorithms are used to approximate galaxy profiles with mathematical functions. Input images from the object of interest must be provided to the programmes together with a desired fitting profile (e.g. the single Sérsic profile). The result is the most appropriate fit of the given mathematical function to the pixel distribution in the input imaging data. The difference between the original image and the fit profile is shown in a residual image by both algorithms. As a result, the residual image provides information on the quality of the fit. In addition to GIM2D, a wide set of mathematical profiles can be applied for the fitting by GALFIT. As a first, but yet still most important step, GALFIT allows for an arbitrary number of Sérsic components in order to fit a galaxy profile. This approach allows to disentangle the multiple galaxy components, such as bulges, disks or bars and to quantify their structures. The user has free control over each profile parameter, such as object position, magnitude, half–light radius, Sérsic index, ellipticity and position angle, in order to keep each component free or fixed to a certain value. Additionally, GALFIT allows for a versatile set of analytical profiles which are suited to quantify a wide range of morphological characteristics such as bars, spiral arms or truncated profiles. GALFIT provides sophisticated concepts for the inclusion or exclusion of neighbouring objects into the fitting procedure as necessary. The latest version of GALFIT, namely GALFITM [Häußler et al., 2013], is able to make use of input images of one galaxy in multiple wavelength bands simultaneously which are provided by large optical and near–infrared imaging surveys. This technique is shown to increase the robustness and the stability of the structural parameters significantly and allows for the study of the transitions in the morphological properties with the change in wavelength.

A detailed comparison between GIM2D and GALFIT by Häußler et al. [2007], which is based on image simulations, has shown that both codes provide reliable fitting results for galaxies with an effective surface brightness brighter than the sky. In contrast to GIM2D, GALFIT is shown to provide more robust results in presence of neighbouring objects and a significantly faster runtime speed are the advantages of GALFIT.

The above described data pipelines can only be used to analyse a relatively small number of objects within one program run. One of the most breakthrough steps in the automated and statistical analysis of galaxy profiles for a large number of objects in imaging surveys has been provided by the first version of GALAPAGOS in 2009 by Barden et al. [2012].

GALAPAGOS can analyse a complete set of imaging surveys automatically without user interaction. It uses SOURCE EXTRACTOR [Bertin and Arnouts, 1996] in order to detect sources automatically. Repeatedly detected sources from overlapping image tiles are erased automatically. It extracts an image region with the object (postage stamp) for each source, automatically calculates a local sky background level and constructs an object mask for each source. Based on this information, GALAPAGOS executes in–depth profile analyses by single Sérsic profile fitting with GALFIT. Finally, the light profile information is collected into a combined output catalogue. Hence, the acronym GALAPAGOS stands for "Galaxy Analysis over Large Areas: Parameter Assessment by GALFITting Objects from SExtractor". However, the fitting analysis with single Sérsic profiles for a large number of objects in modern survey data sets has put the code to its limits and the implementation of more sophisticated fitting profiles is not possible in GALAPAGOS.

At the same time, modern parallelization concepts allow for the implementation of galaxy fitting pipelines on supercomputers. Thus, the present version of GALAPAGOS-C is re–written in C and includes the concepts of the former version of GALAPAGOS. The computation power of modern supercomputers allows for the inclusion of more sophisticated light profiles in the fitting with GALFIT in addition for a large number of galaxies within sensible timescales. As a result, GALAPAGOS-C enables deeper insights into the structure and the evolution of galaxies and their various components. This work describes the concepts of GALAPAGOS-C and its first scientific results.

1.3 The Hubble Space Telescope

1.3.1 Overview of the Technical Facts

The Hubble Space Telescope (HST) was developed as a collaborative project between NASA and ESA and it is named after the famous astronomer Edwin Hubble. Its observation spectrum reaches from the ultraviolet over the visual bands to the infrared. It is the first part of a pioneering mission of four space–based telescopes in the framework of the "Great Observatory Program". The remaining three telescopes are the Compton Gamma Ray Observatory, the Chandra X–Ray Observatory and the Spitzer Space Telescope. After the first light in 1990, it quickly turned out that the HST mirror was incorrectly produced. In 1993, the COSTAR mirror system allowed for a successful correction of the error and further service missions guaranteed for a accurate observational data.

The optical system (Optical Telescope Assembly) is a Ritchey–Chrétien–Cassegrain–construction, which consists of two mirrors. The hyperbolic–formed primary mirror collects the light within a diameter of 2.4 m. The impinging light is reflected to a 30 cm secondary mirror and back to the scientific devices. Five instruments are implemented into the HST. The fundamental device for each of the applications in this work is the Advanced Camera for Surveys (ACS), which is used for wide–area observations in the visible, the ultraviolet and the near–infrared. The high performance ACS is used for the observation of galaxies and galaxy clusters in the local and the distant universe. It consists of three sub–systems: A high–resolution channel, a channel for wide–area applications and a channel for observations in the ultraviolet wavelengths. Depending on the channel, the resolution of the ACS is between ~ 0.03 arcsec/pixel and ~ 0.05 arcsec/pixel. Due to its high resolution, the HST must be adjusted very precisely and the tracking of each object is very sophisticated. It can be adjusted with an accuracy of 0.01 arcseconds and is able to observe an object with an accuracy of 0.007 arc–seconds within 24 h. Due to high temperature variations from the Earth's shadow to sunlit areas, the HST must overcome thermal strain with high–tech isolation material.

1.3.2 Scientific Background

The flagship mission of HST heralded a new era of space–based observation with an unforeseen resolution. As an efficient tool of in–depth observation, it has revolutionized modern astronomy. Even for billions of light–years, the universe is transparent for photons at each wavelength. However, in the last few microseconds before the photons reach the Earth's surface, the visible light is tremendously blurred by the turbulent atmospheric seeing. The ultraviolet and infrared wavelengths are even more affected by this problem. Modern ground–based telescopes can only overcome this problem to a limited extend by adaptive optics and technical adaptation. As a consequence, the vantage point of the HST is chosen to be located at 600 km above the Earth's surface. This allows for the detection of 5 times fainter sources in comparison to the best ground–based telescopes. As a result, modern space–based devices provide insights into the fundamental questions of the universe and allow for pioneering discoveries in modern astronomy.

Fig. 1.6 provides an example for the image quality of one of the HST cameras. In the left image, stars in the Milky Way are taken with the 100–inch telescope at the Las Campanas Observatory, Chile. The smearing by the atmosphere causes optical perturbations and the stars appear blurred and fuzzy. On the other side, the HST data provides well–resolved images for the same cutout of the sky and allows for deeper

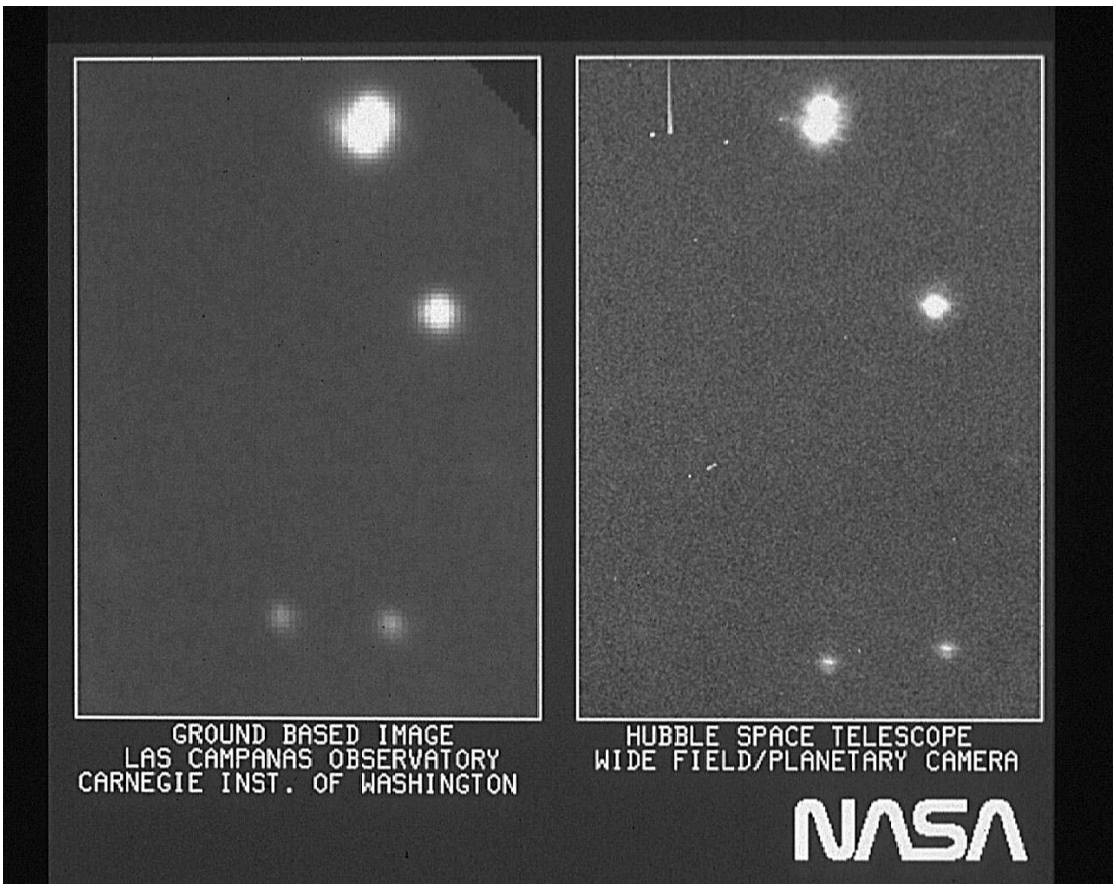

FIGURE 1.6: Illustration of the HST resolution. The right image shows the first image, which has been acquired by the Hubble Space Telescope's Wide Field Planetary Camera in an early engineering state. For a comparison, the same cutout of the sky on the left is taken with the ground–based 100–inch telescope at the Las Campanas Observatory, Chile. The ground–based image illustrates an example for high–quality data. Despite adaptive optics and technical corrections, the objects on the left appear blurred and fuzzy due to the smearing by the atmosphere. Avoiding the smearing by the Earth's atmosphere, the HST observation provides well resolved and sharp objects. The shown objects are stars which are located in the Milky Way galaxy. The uppermost object provides an example for a well–resolved double star system by the HST. This image is an open source illustration by NASA.

insights by resolving even the overlapping neighbouring double star system at the top of the image.

The HST has revolutionized several branches of astronomy. In extragalactic astronomy, it allows for unforeseen insights into the properties of distant galaxies far beyond the precedent observations. For instance, it allows for a better resolution of the components of each galaxy. Second, measuring the distribution of mass in galaxy clusters is challenging. HST observations have been used to map the mass within a galaxy cluster with an unprecedented precision. Also, the HST allows for deep insights and conclusions into the driving processes of interacting galaxies. Fig. 1.7 illustrates examples for interacting galaxies. High–resolved observations open a new window into the associated features,

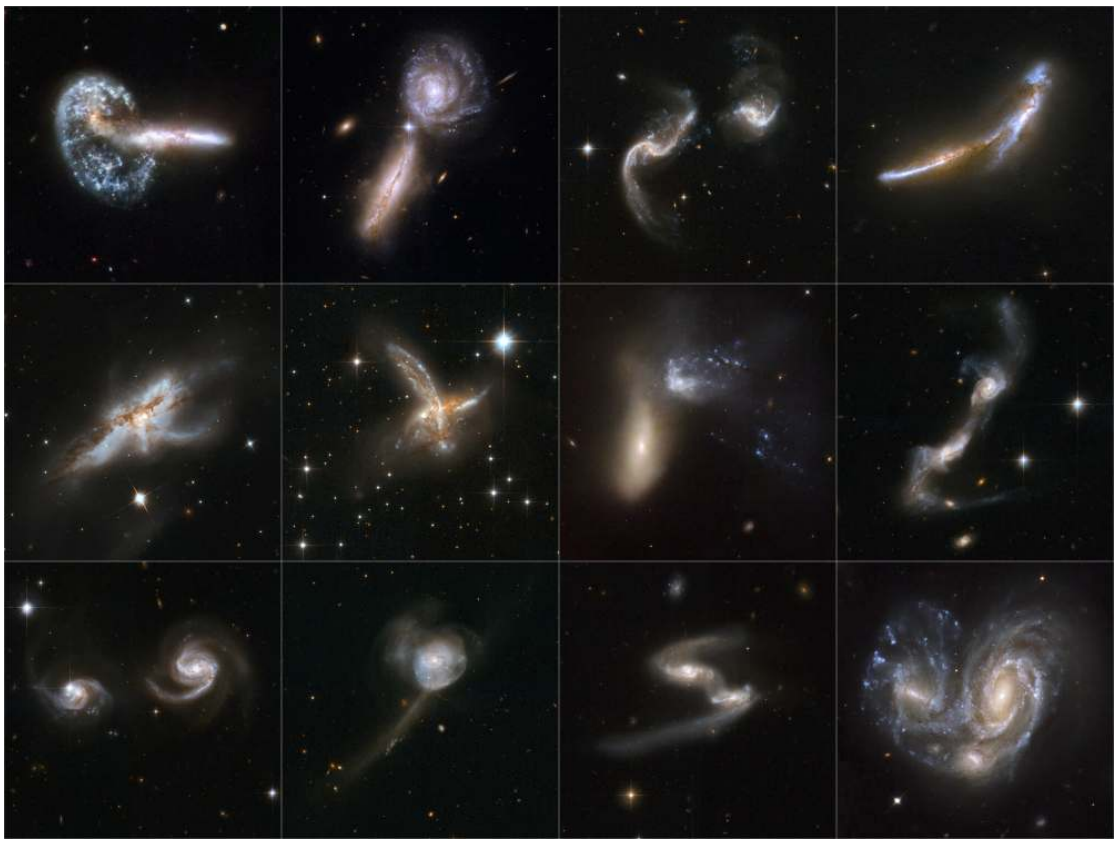

FIGURE 1.7: Prominent images of colliding galaxies at various stages in their merging process taken with the Hubble Space Telescope. The shown galaxies are examples from the new Hubble atlas of galaxy mergers, where the process of galaxy merging with a wide variety of complex structures is shown in an unprecedented detail. This image is kindly provided by NASA.

such as tidal tails, wraps and morphological distortions amongst the involved galaxies. These observational hints and effects provide a key role in our understanding of processes amongst interacting galaxies. Further, its high resolution allows for more precise measurements of the radial velocities of the galaxy and as a consequence for a more precise measure of the Hubble constant and the age of the universe. Prominent examples are in–depth observations of the Hubble Deep Field or the Hubble Ultra Deep Field. Distant supernovae are a suitable tool for the investigation of the expanding universe and provide further hints on the nature of dark matter and dark energy. The HST data helps to prove the existence of supermassive black holes (SMBH) in the centres of many galaxies and provides deeper insights on the effects of black holes on the morphology and the evolution of galaxy structures.

During its lifetime, the HST has produced dozens of terabytes of data as a basis for more than 10000 published papers. As a result, the HST has become one of a the most productive scientific devices of all time.

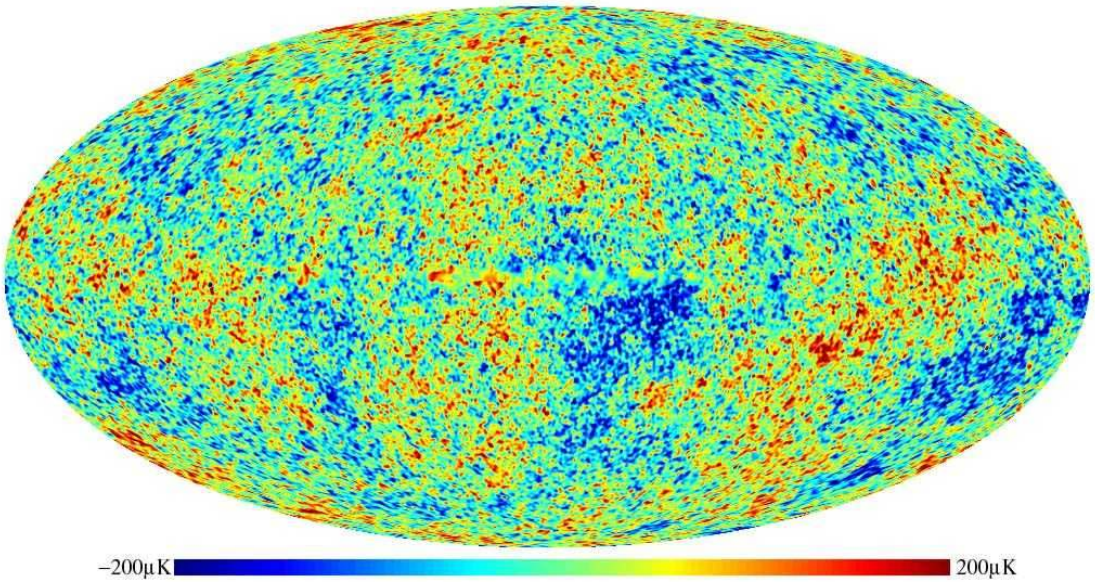

FIGURE 1.8: Illustration of the cosmic microwave background. Temperature fluctuations in the cosmic background radiation are indicated by the color. This image has been aquired by the WMAP mission (2001–2010). Credit: NASA / WMAP Science Team WMAP # 121238 Image Caption 9 year WMAP image of background cosmic radiation (2012).

1.4 Physical Processes in Galaxies and Galaxy Evolution

1.4.1 Overview of the Formation Mechanisms

The formation and evolution of galaxies with their morphological structures is still one of the most important, unresolved questions in modern astronomy. One approach to this question is the statistical analysis of structural, morphological and kinematic parameters for large galaxy samples. One result is that the distribution of galaxy types in the universe is bimodal: One population is observed which consists of early–type, passive galaxies with a spheriodal morphology, an old, red stellar population, no or little cold gas and a relatively slow rotation velocity amongst other intrinsic properties. The counterpart are disk–dominated systems with a younger stellar population, abundant cold gas, active star formation, a faster rotation velocity and blue color. This distribution is known as the 'red sequence' in the former case and the 'blue cloud' in the latter case. In addition, the 'green valley' population consists of a relatively few number of galaxies in between those two accumulation points as an intermediate or transitional state.

Galaxy structures are supposed to arise from an interplay of internal and external physical processes. A large fraction of the galaxy mass is made from dark matter which can only be observed indirectly due to its gravitational interactions. Numerical simulations show that the kinematics and internal structures of galaxies cannot be explained based

on the visible, baryonic mass only. It has been shown that the intrinsic properties and the morphologies of galaxies are strongly correlated with three intrinsic parameters [e.g. Conselice, 2006].

1. The most important parameter is the stellar mass of the galaxy with late–type spiral galaxies and dwarf galaxies on the low mass end and elliptical galaxies on the high mass end.
2. Second, the star formation rate of a galaxies is shown to correlate strongly with the two populations and the morphology.
3. Third, with the pioneering work of Dressler [1980], it has first been shown that local environmental effects and the rate of environmental interactions represent a key parameter in our understanding of galaxy morphology and galaxy evolution.

The Morphology–Density Relation provides information about the relative fractions of galaxy types as a function of the environment. The population in dense environments like the central regions of galaxy clusters is dominated by bulge–dominated systems and disk–dominated galaxies predominantly occur in sparse regions. This finding suggests the scenario of hierarchical mass growth in the universe, which is driven by cold dark matter.

The cold dark matter theory supports a scenario, where structures in the universe grow hierarchically. This means, in general, that the structures in the universe are attracted by their own gravity, collide and merge together in order to form bigger and more massive objects. Fig. 1.8 shows one of the most detailed observations of the cosmic microwave background from modern radio observations. Small local wavelength fluctuations reflect temperature variations and local matter over– and under–densities in the early universe at a relatively short time after the Big Bang. These small over–densities have been collapsing under their self–gravity and merging processes with neighbouring objects result in a continuous growth into more massive objects. As a result, massive, early–type galaxies are mainly the product of major galaxy collisions (mergers).

To that end, the morphology of galaxies must be understood as a result of an interplay of different internal and external processes. Fig. 1.9 shows an overview of the most important processes. According to their relative importance with cosmological time, the processes are arranged from past–dominate, rapid mechanisms on the top to slower processes which predominately occur in the present and the future universe. The early universe is dominated by galaxy formation mechanisms and violent environmental interaction processes. In dense environments and galaxy clusters a variety of interaction processes affect the morphology and the structural properties of the involved galaxies.

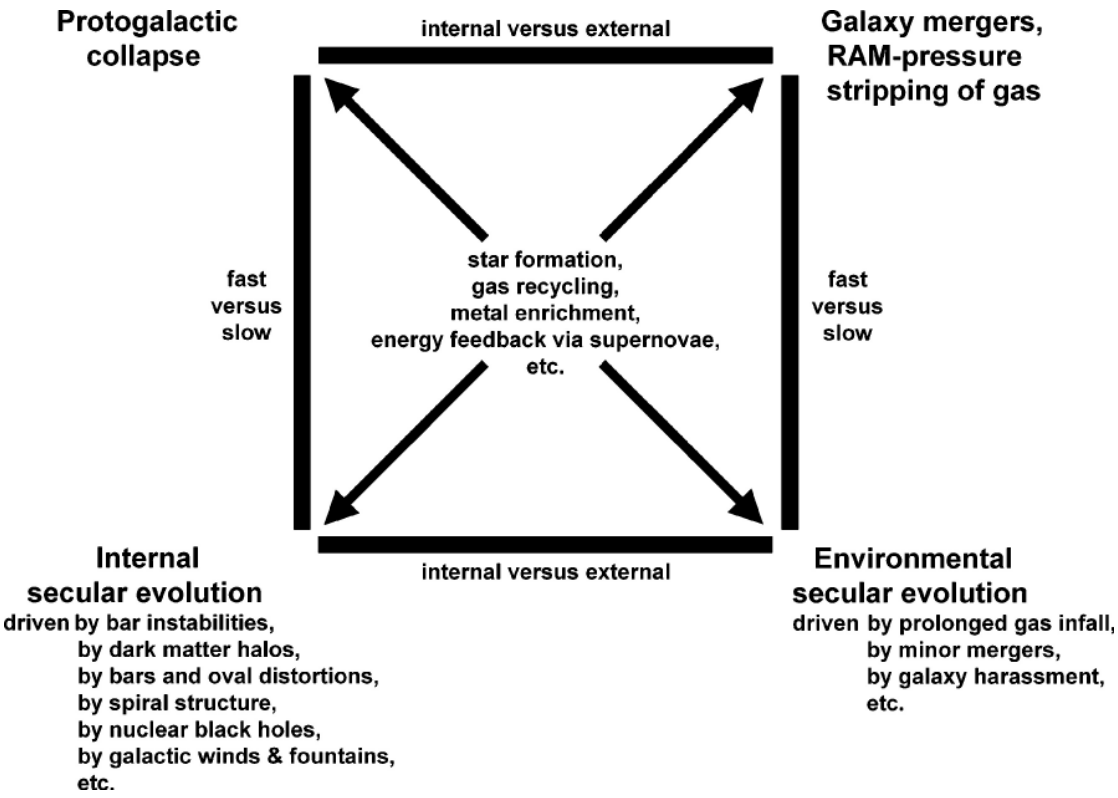

FIGURE 1.9: The 'Morphological box' according to Zwicky [1957] and updated by Kormendy and Kennicutt [2004]. The box provides an overview of fast and slow processes (top vs. bottom) and internal and external processes (left vs. right) as the driving forces for the morphology and the evolution of galaxies. The processes in the centre are related to all categories of galactic processes.

Typical, cluster–specific processes are ram pressure stripping, high–speed fly–by's, harassment, strangulation, starvation, amongst others. Observations show that infalling cluster galaxies are accelerated by the gravitation of a brightest cluster galaxy (BCG) in the centre of a galaxy cluster.

Ram–pressure stripping [Steinhauser et al., 2012, e.g] is a distinctive process in galaxy clusters which triggers or mainly suppresses star formation and thus induces changes in the morphology of a galaxy on the long term. Motions of galaxies through the intra–cluster medium (ICM) at high velocities induce ram–pressure ($\sim \rho\nu^2$) on the gas in a galaxy [e.g. Quilis et al., 2000]. In order to affect the contained gas, the ram–pressure must be strong enough to overcome the potentially existing dark matter halo and the galactic potential well. On short time–scales, star formation can be induced locally [Steinhauser et al., 2012, e.g], but on longer time–scales, the star formation gets quenched due to the gas removal. Intrinsic properties such as the color of the galaxy and the distribution of the stellar matter can be affected in such cases, thus influencing the emergent Hubble type. In the case of spiral galaxies with a lower mass in comparison to ellipticals, the outer regions are gravitationally less bound and thus more sensitive

to soft environmental interaction processes. If the intensity of ram–pressure is lower, it can only affect the gravitationally less bound parts and the interactions with the ICM affect mainly the galactic halo. This process is known as galaxy strangulation or galaxy starvation [e.g. Bekki et al., 2002]. Galaxy strangulation leads to internal, tidal effects in the affected galaxy and ends up with a removal of galactic gas which leads to a suppressed star formation in a similar way.

Morphological distortions of galaxies usually occur in the form of asymmetric or lopsided features and can be accompanied by tidal tails or warps. Such distortions among neighbouring galaxies are often caused by close spatial encounters and indicate interaction processes. In the inner regions of galaxy clusters, the relative velocities amongst the cluster galaxies are generally higher due to the accelerated motions towards a brightest cluster galaxy (BCG) which is located in the centre of the galaxy cluster. In these dense core regions, the relative velocities are too high for galaxy mergers to occur and the involved galaxies are successively exposed to fly–bys from other cluster members. The resulting process is called galaxy harassment [e.g. Gunn and Gott, 1972, Moore et al., 1996]. Tidal forces in the potential wells of the involved galaxies often lead to strong distortions in their morphology, e.g. tidal tails, warps or asymmetries. The overall stellar and gas distribution across a whole galaxy can be radically disturbed and changed. Thus, galaxy harassment can induce short bursts of star formation or even change the Hubble type of a galaxy.

Collisions and merging of galaxies are the most important transformation processes in environments with lower relative velocities. Environments with lower relative galaxy velocities are the peripheral regions of galaxy clusters, galaxy groups or pairs of galaxies. In the case of spiral galaxies, mergers are the most efficient mechanism in order to transform late–type galaxies into ellipticals [e.g. Toomre and Toomre, 1972].

Even if galaxies are not exposed to interaction processes, internal physical processes lead to ongoing changes in the morphological properties. Ageing processes in the stellar populations lead to ongoing structural changes. Supernovae can produce internal shock waves and galactic winds. Re–arrangement of angular momentum can induce secular evolution processes. A prominent, but not yet fully understood, process is the formation of pseudo–bulges. These bulges appear similar to classical bulges, but with circularly orbiting stars. In addition, the stellar distribution of a significant fraction of the disk components show truncations or anti–truncations without environmental dependence. Statistical studies of galaxy–clusters show that $\sim 50\%$ of the spiral galaxies show morphological distortions in the external disk regions independently from interaction processes [e.g. Maltby et al., 2012].

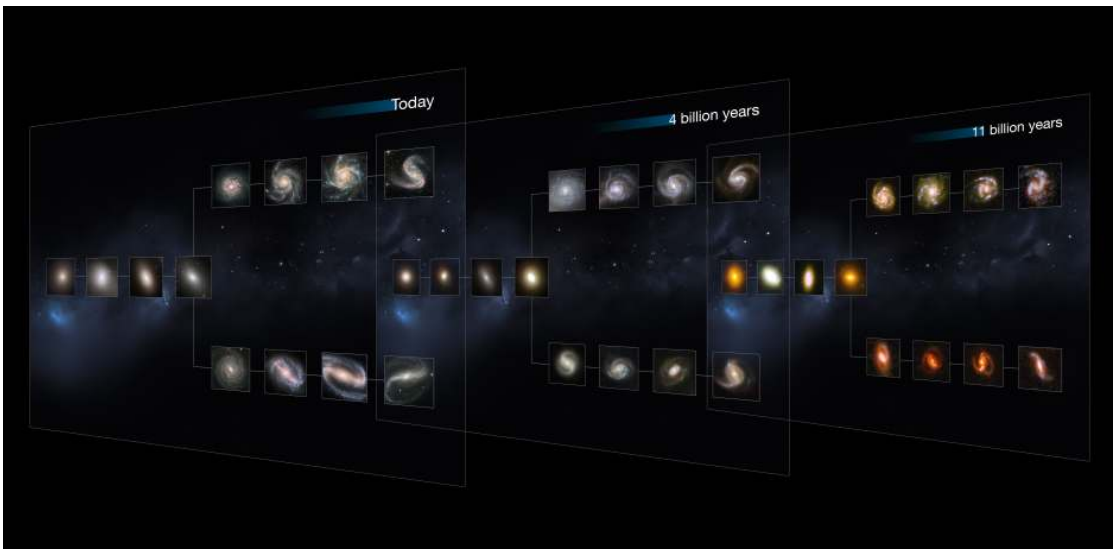

FIGURE 1.10: An illustrative representation of the Hubble Tuning Fork at different times throughout the history of the universe from M. Kornmesser (NASA, ESA). The arrangements according to the morphologies of each galaxy coincide with the standard Hubble Tuning Fork in Fig. 1.2. On the left side, each diagram show elliptical galaxies (E), lenticulars (S0) are again shown in the middle and non–barred spiral galaxies (S) are in the top panels on the right side. Bared spirals are located at the bottom branches on the right. Big, distinct, devoured and fully formed galaxies shapes are found in the present–day universe. Further back in time, the process of galaxy formation is indicated by smaller, more irregular shapes.

A further key role in this context is the impact of SMBH on the galaxy morphology. The majority of bulges and elliptical galaxies are shown to contain a SMBH. Black holes per definition cannot be observed directly, but are rather indirectly observed due to gravitational interaction with neighbouring matter. Further observations have provided information on the activity of black holes, the feedback of active galactic nuclei (AGN) and the accretion of matter around a nuclear black hole and indicate an important role in the mechanisms of galaxy formation and galaxy evolution. A complete theory on the role of SMBH in this context is missing up to date.

The relative importance of the above described processes have been changing over cosmic time. As a result, the observed morphologies and intrinsic properties of galaxies change with further look back into the early universe at higher redshift. Fig. 1.10 illustrates exemplary how the morphologies along the Hubble tuning fork change with cosmic time. Comparable galaxies types in the early universe are on average more luminous due to a higher star formation rate and a higher fraction of young and bright stars with a relatively short lifetime. In comparison to the early universe, the present–day galaxies consist of bigger, distincter and more mature shapes.

While a wide range of processes and evolutionary scenarios have been understood and described in the past decades, the most fundamental questions about galaxy formation

and galaxy evolution remain only partially answered.

1.4.2 The Formation of Disks

Disk components of galaxies are relatively fragile objects and can be easily destroyed by mergers with other, massive galaxies. A first scenario of disk formation was first proposed by Eggen et al. [1962]. In this first theory, the formation of disks was caused by a monolithic collapse of a gas cloud and the conservation of rotation momentum (top–down formation scenario). However, observations of the early universe strongly suggest that structures are merging from small, bound assemblies towards larger structures (bottom–up scenario) [Searle and Zinn, 1978]. Kinematic analysis of disk galaxies show that disks should be temporarily unstable if the motions were only gravitationally driven by the visible, baryonic matter. A key role in this context is the presence of dark matter in galaxies and dark matter halos. In disk galaxies, gas is observed to contract and form stars and thus dissipate. Dark matter is suggested to slow down the gas contraction in the disk and to keep the gas on stable orbits inside the galaxy on a thin, rotating disk which is temporarily more stable. In addition, this ongoing process is often provided with further matter due to minor mergers with smaller satellite galaxies. Such mergers provide new angular momentum, gas, stars and dark matter to the disks. The physical details of the disk formation scenarios and the role of dark matter in this context are still not understood completely.

1.5 Intention of this Thesis

The intention of this thesis is twofold: First, the computational means for the automated analysis of large survey data, GALAPAGOS-C, is presented in detail. A systematic insight shall be provided in the structure of the code itself, tests on the stability, the data reliability and the speed–up performance of GALAPAGOS-C. The second part deals with scientific applications of GALAPAGOS-C. The morphologies of a large number of sources in the Hubble Space Telescope (HST) surveys STAGES and GEMS shall be quantified. GALAPAGOS-C provides new approaches in order to analyse imaging survey data in an unforeseen scale and new aspects on studying the distribution and evolution of galaxy morphologies are presented. In detail, robust statistics on the distribution of Sérsic profiles and morphological structures of galaxies in the A901/902 galaxy cluster shell be provided. In addition, Fourier mode fitting allows for a first automated quantification of morphological distortions in the galaxy cluster for a large number of cluster member galaxies and galaxies in the field. The intensity of morphological distortions and asymmetries shell be quantified with regard to the correlation with other structural and

intrinsic galaxy parameters, such as distance to the cluster centre, stellar mass or color. The GEMS survey provides a wide sample for measuring the evolution of morphological distortions and galaxy asymmetries in the field.

The presented calculations are based on the ΛCDM model of cosmology with the parameters $H_0 = 74.3\ \mathrm{km\,s^{-1}Mpc^{-1}}$, $\Omega_M = 0.286$, $\Omega_{vac} = 0.714$.